CONF-9510358--1

Advancing Manufacturing Through Computational Chemistry

Donald W. Noid, Bobby G. Sumpter, Robert E. Tuzun
Chemical and Analytical Science Division
Oak Ridge National Laboratory
Oak Ridge, TN 37831-6197

Abstract

The capabilities of nanotechnology and computational chemistry are reaching a point of convergence. New computer hardware and novel computational methods have created opportunities to test proposed nanometer-scale devices, investigate molecular manufacturing and model and predict properties of new materials. Experimental methods are also beginning to provide new capabilities that make the possibility of manufacturing various devices with atomic precision tangible. In this paper, we will discuss some of the novel computational methods we have used in molecular dynamics simulations of polymer processes, neural network predictions of new materials, and simulations of proposed nano-bearings and fluid dynamics in nano-sized devices.

I. INTRODUCTION

Recent progress toward miniaturization has demanded new ways of thinking about mechanical devices. This is particularly true in the technologies of sensors-on-a-chip and information storage, where micro-electromechanical systems (MEMS) are recognized as major, new areas for development [1]. The logical extension of this technology is into the area of nano-scale devices such as bearings and gears, in which the whole component is comprised of only a few thousand or million of atoms. This area of study, often referred to as molecular nanotechnology, has the potential to revolutionize chemistry, materials science, biology and many other fields by creating an entirely new set of atomically precise mechanical devices and molecular machines. Molecular nanotechnology proposes to exploit this fundamental knowledge by using a bottom-up approach to constructing nano-scaled objects, that is, assembling components atom-by-atom.

While molecular nanotechnology is not a present reality, the surprising capabilities of the Atomic Force Microscope, laser lithothgraphy and the optical tweezers give credibility to predictions of molecular control of complex structures near its atomic limit. Recently K. E. Drexler has discussed this ultimate capability in *Nanosystems: Molecular Machinery Manufacturing and Computation* [2]. The main premise of that work is that any arrangement of atoms that is consistent with the laws of chemistry and physics can (or will) be assembled (on an atomic scale). Based on this thesis, Drexler and R. C. Merkle [3] have proposed a number of possible designs that represent essential components of machines that perform specific operations. One proposed method to manufacture these new tools involves using mechanosynthesis or mechanically guided chemical reactions. The concept of positionally controlled chemical reactions may create another novel application for the atomic force microscope. Several other conceptual techniques for molecular manufacturing have also been proposed.

Simulation of the internal dynamics and performance of molecular-based materials will provide much of the needed data for developing and testing fundamental concepts and designs of nano-machines or components. However, in order to examine details pertaining to the operation of such devices, the simulation time and size must sample that comparable to the object and its expected operation time. Thus, it is clear that new avenues to the molecular dynamics (MD) method, which has traditionally been plagued by exactly this size-time scale bottleneck, are needed to make the fundamental foundation of the method useful. Fortunately a great amount of effort has been expended to eliminate this problem. Probably the most dramatic increase in capability on the computational side is the development of massively parallel computers such as the Intel Paragon, Cray T3D, etc. The arrival of these computers has been accompanied by development of several very powerful message passing algorithms for sharing out the computational tasks among the large number of CPU's. Various research

groups have very recently demonstrated molecular dynamics simulations with up to a billion (10^9) [4] atoms and it appears that this limit is being rapidly increased. One billion atoms would encompass approximately a cube on the order of 0.1 micron or 100nm per side. This is a size scale that can be easily manipulated with current technologies.

Our computational chemistry work at ORNL has focused on development of techniques that are applicable to workstations for performing molecular dynamics on smaller systems or components of nanomachines, the solution to the problem that very long simulations may be required, high resolution spectral analysis and data extraction methods and the use of computational neural networks to design new materials, optimize the performance of processes important to nanotechnology, and to perform automatic data clustering and classification. In this paper we will discuss three of these methods: geometric statement functions (for producing faster MD codes), symplectic integration (for generating stable long time trajectories), and computational neural networks. An important aspect of these techniques is that the simulations are very efficient (orders of magnitude faster than previous methods) and exact (classical constants of the motion, such as energy and momentum, are conserved) for indefinite periods of time. In the next section a brief description of our developments of molecular dynamics techniques and a computational paradigm using neural networks to optimize materials is given. In the final section we present results from some recent molecular dynamics simulation of bearings, motors and fluid flow on the nanometer scale.

II. SIMULATION METHODS

MOLECULAR DYNAMICS

Molecular dynamics (MD) simulations provide an important tool for investigating fundamental processes in many areas of chemical physics, macro-molecular chemistry and molecular nanotechnology. We are particularly interested in large scale MD simulations involving thousands of atoms, over very long time scales. There are a number of reviews available [5] that discuss the fundamentals of classical MD techniques. In short, MD simulations involve first setting up the initial geometry and velocities of the particles, and then the numerical integration of the classical equations of motion. Numerical integration is the most computationally intensive part of a MD simulation. As the number of particles in a simulation increases, the numerical integration can represent a severe bottleneck to progress. Numerical integration routines generally require a number of force evaluations, i.e., evaluations of the negative gradient of the potential, in order to advance a trajectory by a given time step. The computational effort is usually proportional to the number of force evaluations.

A common numerical integration algorithm in MD simulations is the Verlet method. It has the advantage of being easy to program and is very robust, i.e, it can generate stable, long time trajectories. Although the Verlet method is a symplectic integrator (SI), its accuracy is of too low an order for our work. SI's are special algorithms for solving the classical equations of motion (Hamilton's equations) that are guaranteed to preserve certain dynamical properties that exact trajectories are know to exhibit. Over the past ten years there has been an explosion of research into SI's, mostly in areas of few body simulation of interest to astronomy and other fields [6]. It has often been demonstrated that SI's provide reliable long time trajectories which exhibit features typical of the true dynamics. It is also anticipated that some SI's should be more efficient than other, more standard numerical methods of solving the classical equations of motion.

The classical equations of motion can be written as a Hamiltonian system of ordinary differential equations,

$$\cdot\ \partial p_i/\partial t = -\partial H/\partial q_i \qquad \partial q_i/\partial t = \partial H/\partial p_i$$

where $(q_i,p_i), i=1,\ldots,N$ is a set of N canonically conjugate vector Cartesian coordinates and momenta, and H is the classical Hamiltonian. Unlike many numerical methods for solving sets of ordinary differential equations, e.g., standard Runge-Kutta algorithms, SIs are specifically tailored to Hamiltonian systems because they satisfy the symplectic property that exact solutions must satisfy. In a recent article we explored and extended the use of these methods for large scale molecular dynamics simulations. This extension helped in the elimination of a start up error, which occurs because of the way kinetic energy is added to the system being studied. It was also about a order of magnitude more accurate for the same step size in the integration procedure. A more complete discussion of SI's can be found in reference 7.

Although the vector equation above appears simple, it actually represents 6 equations for each atom (i.e. for 1 million atoms one would need to solve 6 million nonlinear ODE's!). Because the equations are usually written in Cartesian coordinates the second equation is relatively simple. Unfortunately this is not true for the first equation since the potential energy function is written in internal coordinates (bond stretches, bends, torsions and wags). The first equation therefore involves a large number of algebraically tedious equations. Some of these equations require as much as 30 lines of FORTRAN code. Several years ago we developed a solution to this problem which reduced the computational effort by about a factor of 30-50. This solution involved (a) using closure relations among the various derivatives, (b) eliminating a vector cross product by way of one of Lagrange's identities, and (c) reusing two- and three-body coordinates and derivatives as intermediates for calculating three- and four-body terms (which can be easily be accomplished with statement functions, which is why we called this method the geometric statement function approach). Because of space limitations we refer the reader to more complete discussion in reference 8.

COMPUTATIONAL SYNTHESIS: A NEW TECHNIQUE FOR THE DESIGN AND ANALYSIS OF MATERIALS

Up to now materials design and processing have been to a large extent empirical sciences. We are still unable to design new alloys and polymers to meet application specific requirements. Being able to do so quickly and at minimum cost would provide an incredible advantage, subsequently leading to significant advances in quantity and quality of materials products. We have recently developed and tested a method called computational synthesis that provides breakthrough capabilities for addressing this important problem [9]. The method can predict physical, chemical, or mechanical properties of compounds prior to their experimental synthesis or even design chemical structures that meet specified performance criteria. Figure 1 illustrates the fundamental components of the method and compares it to the empirical approach for materials design.

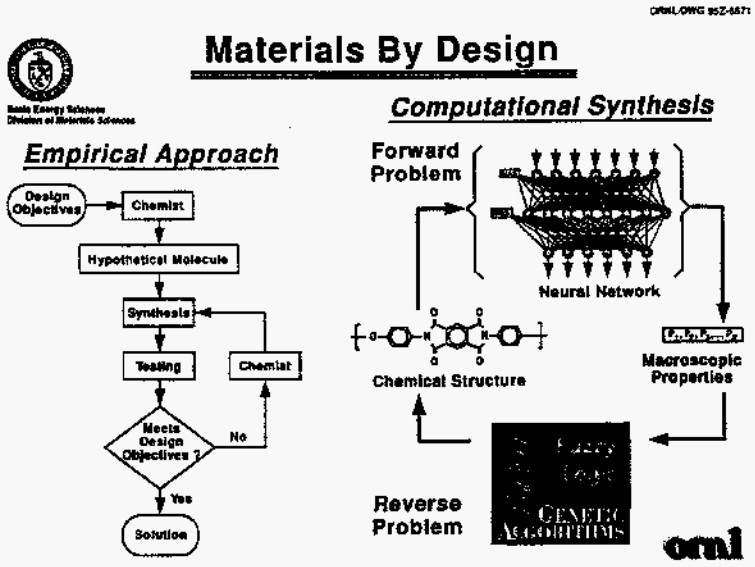

Figure 1. Schematic diagram illustrating the computational synthesis method.

Computational synthesis represents a hybrid of a number of emerging technologies (computational neural networks, graph theory, genetic algorithms, wavelet theory, and fuzzy logic) and has proven to work very well for test compounds ranging from small organic molecules to polymeric materials. The advantage of the

computational synthesis technique is its ease of use, speed and accuracy; it can be used to predict both properties from structure and structure from properties, which opens the door to novel and efficient design of advanced materials. Practical uses of the computational synthesis method could include: (1) examining the feasibility of using a given material for particular applications; (2) testing the long-time performance of crucial properties (as specified by the materials' technological application) for candidate or existing materials; (3) directly assisting in the design of new molecular-based materials with enhanced properties in order to optimize performance; (4) choosing and optimizing processing techniques for generating final products from raw materials.

III NANOTECHNOLOGY SIMULATIONS

NANO BEARINGS, MOTORS AND TRIBOLOGY

Various types of molecular bearings have recently been proposed in the growing nanotechnology literature [10]. Using novel molecular dynamics methods, we have simulated several model graphite bearings [11]. All calculations were performed in double precision on an IBM RS6000 model 580 cluster with 4 CPUs. While diamondoid bearings may behave more ideally than graphite bearings due to their greater stiffness, their construction must await mechanical synthesis or some other innovation. In contrast, nanotubes of graphite have already been synthesized in a variety of sizes and shapes and manipulating them into bearings seems plausible [12]. The bearings that were simulated varied in size from an inner shaft of between 4 and 16 Å in diameter and up to 120 Å in length and an outer cylinder of between 10 and 23 Å in diameter and up to 40 Å in length. The turning shaft was either instantaneously started or was torqued up to the desired rotational speeds. Figure 2 shows the basic construction of a nanobearing at the beginning of a simulation. Both the shaft (inner cylinder) and sleeve (outer cylinder) are centered about a common rotational axis, denoted the z axis, and the shaft extends symmetrically out of the sleeve.

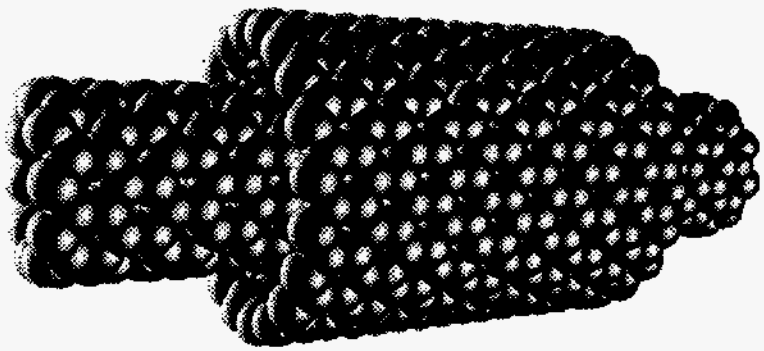

Figure 2. Basic construction of a graphite molecular bearing.

Shaft and sleeve radii, which greatly affect bearing performance, are calculated as follows. The shaft and

sleeve are, respectively, n and m atoms in circumference. From the equilibrium bond distance and bend angle, the distance between the end atoms in a bend interaction is 2.46 Å. The shaft radius is the radius of a regular polygon with n/2 sides of length 2.46 Å. From simple trigonometric identities and the approximation $\sin\theta \approx \theta$ (an approximation accurate to within less than 1% even for the worst case, n = 10), this radius is about $(1.23/2\pi)$ n Å. Thus, the bearing clearance is approximately $(1.23/2\pi)$(m - n) Å. In some simulations a random amount of momentum was added to create a desired temperature. Angular momentum was added to generate rotation about the z axis so that the shaft and sleeve had equal but opposite angular momenta. An example of the performance of a well designed molecular bearing (under no load) is shown in Fig. 3 by the plot of slow loss of angular velocity as a function of time.

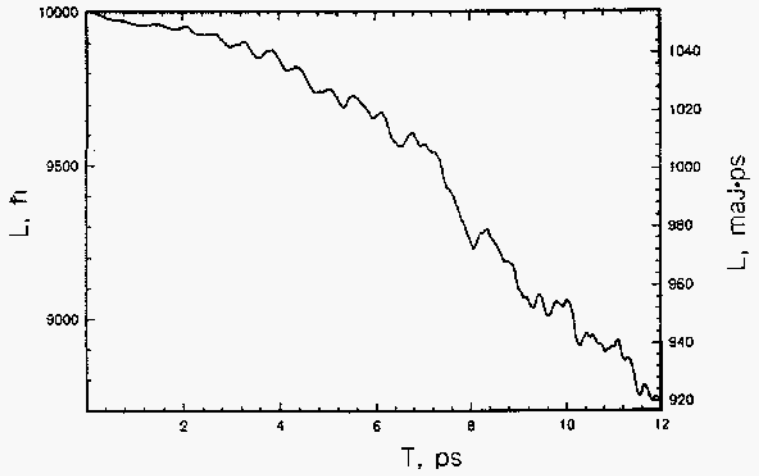

Figure 3. Rotational frictional behavior of a typical graphite molecular bearing.

Initial (2 ps) drag coefficients showed distinct size, velocity, and temperature dependence. As the bearing grew tighter (smaller m - n) or the temperature rose, the drag coefficient increased. In addition, the coefficients were small if the sleeve was frozen during simulation, because no energy could be dissipated into sleeve internal modes. We have found that models must be completely dynamical to properly describe the frictional behavior in molecular bearings. Initial design parameters (bearing clearance, for example) can be roughly modelled with the aid of tools for studying static systems such as molecular mechanics. Bearing clearances must fall in an intermediate range in order to obtain a smooth fit and smooth rotation. Frictional behavior follows expected trends in temperature and rotational velocity.

Results for one particularly interesting simulation are shown in Fig. 4. Initially, the shaft and sleeve are rotated in opposite directions with a rotational velocity corresponding to 10000 $\hbar$ (1054 maJ • ps); no external torque is applied. From the shaft angular momentum in this figure, the first 15 ps of the simulation are similar to those of most of the other simulations in our study: slow, steady loss of angular momentum with fairly small oscillations. Between about 15 ps and 60 ps, however, there are three beats with oscillations of several thousand $\hbar$ (several hundred maJ • ps). After 60 ps, the shaft once again steadily loses angular momentum; however, the oscillations are much larger than in the first 15 ps. At times, the shaft (and therefore the sleeve, since in this case the total angular momentum is zero) briefly reverse direction. We find that the beats arise from the presence of two types of motion, a tube breathing mode in the sleeve and the shaft and sleeve sliding axially

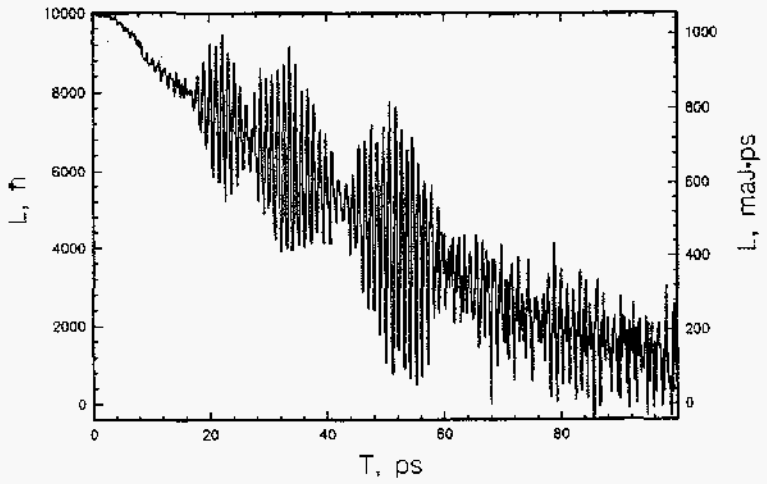

Figure 4. Rotational velocity beat patterns in a graphite molecular bearing.

across one another by one or more rings. After 60 ps, the shaft and sleeve no longer slide across one another, and the beats stop.

Transverse loads can significantly degrade bearing performance if the bearing deforms under shear. In real nano-machines with components such as gears, the transverse load exerted on bearings could have a complicated time dependence. For that reason the dynamics of real nanomachine components would likely be considerably more complicated than those shown here. However, it seems safe to say that bearing components should either be stiff or should be constrained so as to not allow extraneous vibrational effects.

In summary we have found frictional properties to be size-, temperature-, and velocity-dependent. The presence of more than one bearing vibrational mode in some simulations created beats that could possibly adversely affect bearing performance; placing a stretching tension on the bearing suppressed one of the modes and therefore the beats.

The usefulness of studying a molecular bearing has in it the assumption that some kind of device can be built to create mechanical rotational motion. Using molecular dynamics methods, we have proposed and simulated several model graphite nanometer scale laser-driven motors [13]. To our knowledge, this is the first study of laser excitation of a nanometer-scale device and represents a small extension to ideas well known in rotational spectroscopy. These motors consisted of two concentric graphite cylinders (shaft and sleeve) with one positive and one negative electric charge attached to the inner shaft shown in Fig. 5; rotational motion of the shaft was induced by applying one or sometimes two oscillating laser fields.

Since we attempted to model a startup process the shaft was initially motionless. The outer sleeve was frozen throughout the simulation. Calculations were performed for several nanotube sizes and field strengths and frequencies. Typical simulations ran for several hundred ps. Figure 6 shows a typical profile of shaft angular momentum L_z which indicates the rotational velocities created by the laser. Both angular momentum and the absorbed energy show strong beat patterns; in many cases, it cycles between rotational pendulum-like behavior (angular momentum oscillations between positive and negative values) and unidirectional motion (motor-like behavior) in which the oscillations die down and then build up again.

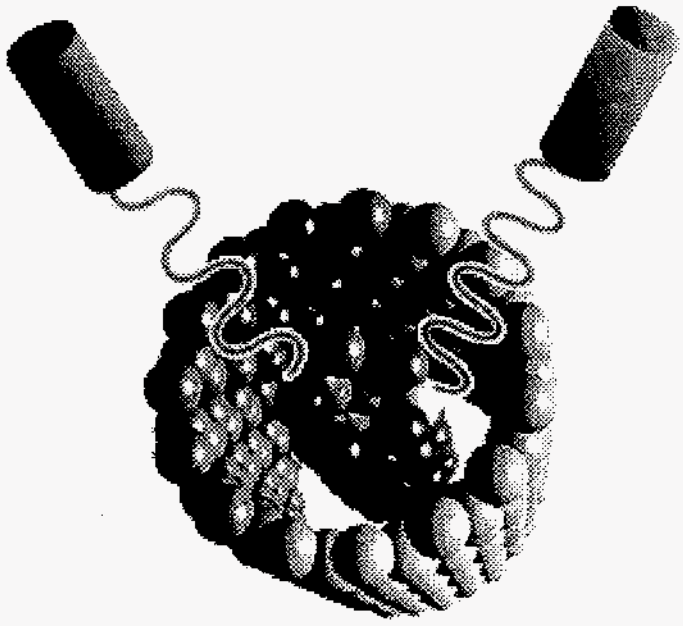

Figure 5. Schematic of a laser-powered graphite molecular motor.

The beat patterns tend to be fairly symmetrical. Most runs show an initial lag time of pendulum-like behavior; this lag time can run up to about half the time for a full cycle of pendulum-like behavior. The performance of motors with the same size and excited with the same frequency varies greatly with the field strength. At low field strengths, the beat patterns are comparatively weak. As the field strength increases to intermediate values, the angular momentum (and total energy) oscillations increase in magnitude. Increasing the field strength above the best performance limit significantly increases beat amplitudes in both the on and off cycles and they become more asymmetrical. In addition, the total energy exhibits a significant positive drift, indicating excitation of internal vibrational modes. It should be noted that the direction of unidirectional rotation may change from one on/off cycle to the next, although its magnitude may not significantly change.

To find the most optimal operating conditions required a more extensive search of parameter space and was accomplished with the aid of neural network methods to "learn" the mapping from size, charge position, frequency and strength of the electric field to the motor on and off times. This multidimensional, nonlinear mapping was determined to within an average accuracy of 2% and could be used to determine initial parameters that would lead to better overall performance of the nanomotor.

In previous laser chemistry applications [14], it was found that two lasers are more efficient for creating vibrational and rotational excitations than a single laser. For this reason and because of the surprising on/off behavior of the one-laser excitations, we performed several two-laser runs. A run for which the second laser field is an overtone of the first and has the same intensity not only greatly enhanced the on/off time ratio, but had much weaker oscillations in both angular momentum and total energy, i.e., more ideal motor performance. When two lasers were slightly detuned from each other, we obtained even better performance.

The use of one- or two-laser excitation of nanometer scale components may prove to be a practical method for introducing controlled motion into nanomachines. With sufficient shaft-sleeve clearance and in the proper regimes of laser field strength and frequency, stable rotational motion was introduced into a model nanometer scale motor at speeds up to about 10^{12} Hz. The shaft of the motor did not significantly distort during simulation, except at the end with attached charges. The induced motion appeared to be almost purely rotational, except at the most intense laser fields. For our simulation purposes, we have used fairly high laser powers in order to

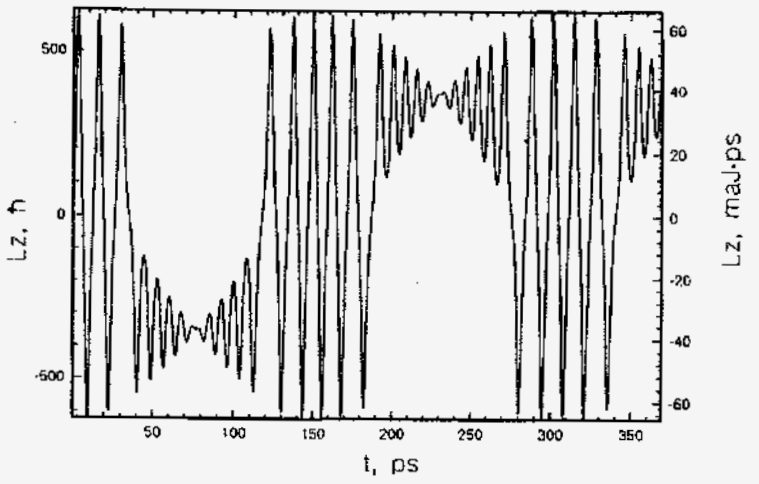

Figure 6. Motor- and pendulum-like motion for a model molecular motor.

fairly quickly excite rotational motion. Similar results could perhaps be obtained with lower powers but for much longer simulation times. We would expect weaker beat patterns and slower induced rotations. The use of two lasers appears to enhance the transfer of laser energy into rotational motion and to induce more stable motion than using one laser. In the two-laser excitation of HF [14], chaotic motion was proposed to be the mechanism for this enhanced excitation. The role of chaos in our model graphite motors and in other nanosystems needs to be studied further.

FLUID DYNAMICS AND MASS TRANSPORT

Gases or liquids that flow through pipes or are confined to small volumes are likely to find a wide variety of applications in nanotechnology, especially in nanomachines with moving parts. For example, they could serve as hydraulic fluids in support platforms. They could also carry reactant molecules into reaction chambers. The behavior of fluids in nanomachines is expected to be fundamentally different from fluid behavior in other systems. Consider, for example, a liquid flowing through a macroscopic pipe. Models of the fluid behavior usually begin with the continuum hypothesis, where one ignores the atomic structure of the fluid and instead characterizes it by viscosity, density, etc. If the flow is laminar, one can calculate the velocity-radius profile. Problems to be solved in this size regime include, for example, calculating power requirements for pumping the fluid through the pipe. The behavior of the pipe itself is usually ignored except to provide boundary conditions. One common boundary condition is the no-slip condition (zero fluid velocity) at the walls. The fluid velocity isn't necessarily zero at the walls; it is simply negligibly small compared to bulk fluid velocities. Although one can explain the validity of the no-slip condition in terms of the behavior of the fluid and pipe at the atomic scale, only the no-slip condition itself, and not the physics behind it, is required for the purpose of engineering design.

Modelling fluid behavior inside nanomachines or components introduces another level of complexity: both the "walls" and fluid can move. Furthermore, the movement of the "walls" is sometimes strongly size-dependent (through normal modes). Design considerations for nanomachines or components in which fluids flow will therefore include both fluid and "wall" effects and their interplay. Such concepts as viscosity and pressure may

sometimes have a narrow range of application and must be applied carefully.

We have simulated the axial flow of He and of Ar through carbon nanotubes, which serve as pipes [16]. The tube is clamped (frozen) at both ends and would be similarly constrained in real nanomachines. Figure 7 shows the fluid and tube at the beginning of a simulation. The fluid begins in a cubic lattice inside the tube; this initial lattice never passes within 2.5 Å of any atom in the tube. The lattice parameter is set according to the desired fluid density. Fluid atoms are allowed to recycle from one end of the tube into the other through minimum image boundary conditions. We carefully considered whether to allow the fluid and tube to equilibrate before giving the fluid a velocity because an initial lattice structure would in some simulations be unrealistic; we found this was unnecessary because the lattice structure was almost always lost within 0.2 or 0.4 ps, a small fraction of the simulation times.

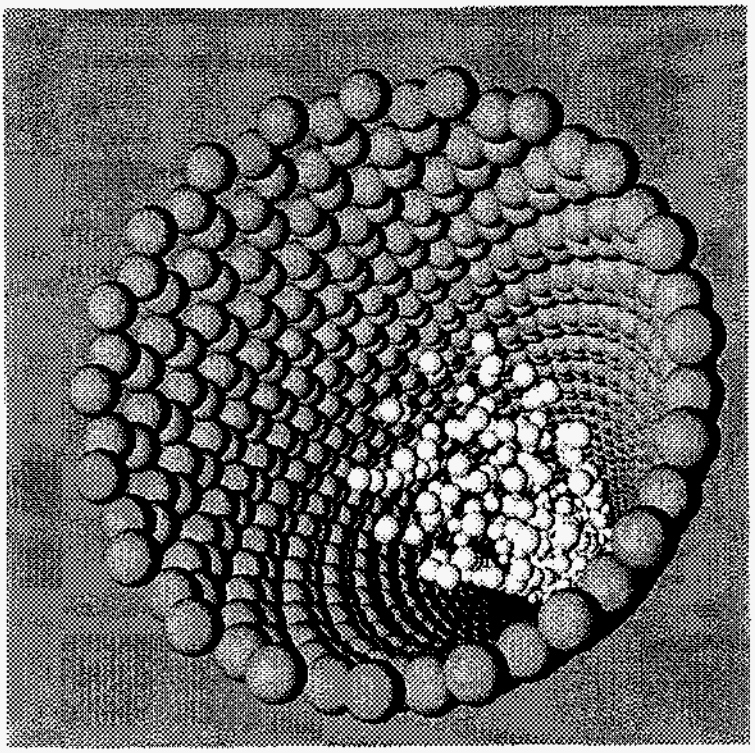

Figure 7. Schematic of fluid flow inside a carbon nanotube.

In a fluid/carbon nanotube system, the motion of the carbon nanotube plays a critical role in fluid flow. In our simulations, the fluid slows down because of fluid-carbon nanotube collisions. If the tube is static, the collisions are more elastic than if the tube is dynamic. In addition, as the tube moves, it jostles the fluid atoms nearest it, causing the fluid motion to randomize more quickly. At equivalent volumetric flow rates and number densities (which can be reasonably approximated from initial fluid atom lattice spacing), a He fluid flows through a carbon nanotube more easily than Ar. This is because Ar is 10 times more massive than He and induces larger amplitude vibrations in the carbon nanotube. The length of the carbon nanotube does not appear to appreciably affect the behavior of the fluid. We have found the nanotube length to affect the dynamics of individual nanotubes and bearings because energy tends to flow into the low-frequency modes, which are size-dependent [15]. By contrast, a fluid flowing through a nanotube excites or deexcites many modes simultaneously and tends to straighten out the tube as it flexes. Thus, modes which include longitudinal motion never get a chance to develop. Since the tube is clamped at both ends, stretch modes do not develop, either. Whether the tube is static or dynamic, the more dense a fluid is, the faster it slows down. This is a straightforward consequence of increased collision frequency. At very low densities, the fluid would not interfere with the development of longitudinal motion in the carbon nanotube, and the length of the tube would likely have some effect on the fluid behavior.

In these simulations, we have concentrated on trends in fluid and wall behavior. We have not calculated

viscosities from our data, nor is it clear how best to define an effective viscosity. Whereas in continuum fluid mechanics viscosity is a property of the fluid alone, in our simulations any definition of effective viscosity would inevitably contain information about fluid-wall interactions. Therefore, in nanotechnology applications any value for effective viscosity must be carefully considered in the context of the system being studied.

In other simulations involving a fluid carrying an idealized buckyball (C_{60}) atom or a fully atomistic buckyball cage [17] (see Fig. 8) the buckyball atom or molecule is initially located at the middle of the buckytube. The initial fluid lattice does not pass within 7 Å in z of the buckyball atom or center of the buckyball cage. The idealized buckyball atom is allowed to cross the minimum image boundaries in the same manner as the fluid. In most simulations, the buckyball atom starts at zero velocity (this is to simulate a situation in which the buckyball atom is introduced into a feedstream). In some simulations, the buckyball atom is started at the initial fluid velocity. In simulations involving the C_{60} cage, the cage atoms cross the minimum image boundary individually; minimum image boundary conditions are accounted for while dealing with stretch or bend interactions within the cage. The C_{60} cage is started at the initial fluid velocity but with no initial rotational or random thermal motion.

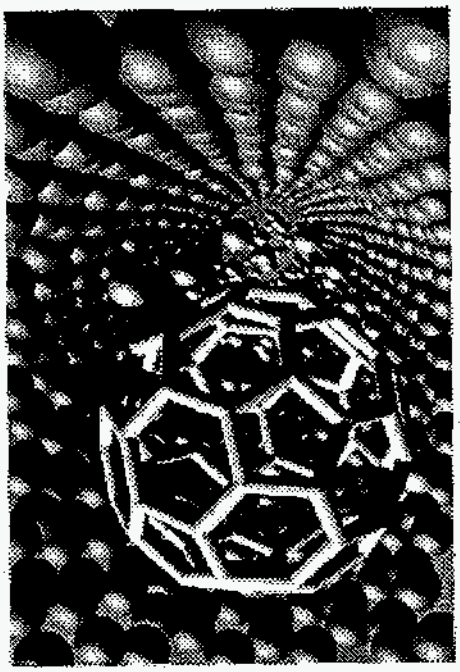

Figure 8. Schematic of He/C_{60} flow inside a carbon nanotube.

The leakage rate of fluid past the buckyball is strongly influenced by the diameter (but not length) of the tube, because the diameter of the buckyball is of the same order of magnitude in this work. Essentially, if there is room for the fluid atoms to leak past the buckyball, some leakage will inevitably occur. The leakage rate is also influenced by how rigidly the carbon nanotube is restrained (if it's held under tension, for example) and the pressure at which the fluid is being pumped. Simulations in which the nanotube is frozen throughout the simulation can exhibit leakage rates several times as large as those in which the tube is dynamic. Because of the minimum image boundary conditions, pressure effects were not explicitly considered here. Such effects (for example, acoustic waves generated by fluctuations in feed pressure) should be carefully considered during the final stages of design for nanomachines involving fluid flow. We have considered two types of situations in which a feedstream of helium carries along a buckyball idealized atom or fully atomistic cage: a buckyball moving at the feedstream velocity or with zero velocity. The zero-velocity case could correspond to a buckyball being introduced into the feedstream. The buckyball atom can restrict the fluid flow cross section and fluid can immediately slow down, depending on the diameter of the feed tube, and thereby create a back-pressure wave.

Design considerations for nanomachines or components in which fluid flow should include the possibility of flow restriction or blockage. Because of its inertia, the buckyball atom takes time to speed up and may never reach the feed stream velocity. If, for example, a nano-reaction vessel were vented, the buckyball would likely exit the reaction vessel or flow out the vent pipe slower than the rest of the fluid, depending on the sizes of the reaction vessel and vent pipe. The non-zero-velocity case could correspond to a large feed stream splitting into several smaller streams. Once inside the smaller pipe, the buckyball could flow along the walls and pass the fluid atoms. We have observed this in our simulations, which involve helium. Similar effects might be smaller if much heavier fluid atoms, such as argon, were used.

Finally we have found the use of animation or movie presentation of the dynamics to be very useful in characterizing the success or failure of the nanotechnology processes being simulated. For example, in our bearing simulations, ring breathing and other tube modes could be directly vizualized. Analysis of MD data is far more illuminating when it is accompanied by visualization.

ACKNOWLEDGEMENTS

This research was sponsored by the Division of Materials Sciences. Office of Basic Energy Sciences, U.S. Department of Energy, under contract DE-AC05-84OR21400 with Lockheed Martin Energy Systems, Inc. In the course of this work we have benefitted from various collaborations S. Gray (symplectic integration methods), R. Merkle (fluid mechanics) and nanotechnology discussions with Prof S Meyer, S Vetter, R Merkle, W King and S. Gray. The animations were created by R Toedte in the ORNL VIZLAB.

REFERENCES

[1] G. Stix, *Scientific American* **267**, 106 (1992).

[2] K. E. Drexler, *Nanosystems: Molecular Machinery, Manufacturing, and Computation*, (John Wiley, New York, 1992).

[3] R. C. Merkle, *Prospects in Nanotechnology*, Ed. M. Krummenaeker and J. Lewis, p23-49 (John Wiley, New York, 1995).

[4] E. F. D'Azevedo and D. W. Walker, *SIAM News*, **28**(5), (1995).

[5] M. L. Klein, *Ann. Rev. Phys. Chem.* **36**, 525 (1985); W. G. Hoover, *Ann. Rev. Phys. Chem.* **34**, 103 (1983).

[6] M. P. Calvo and J. M. Sanz-Serna, *SIAM J. Sci. Comput.* **14**, 936 (1993).

[7] S. K. Gray, D. W. Noid, and B. G. Sumpter, *J. Chem. Phys.* **101**, 4062 (1994).

[8] D. W. Noid, B. G. Sumpter, B. Wunderlich, and G. A. Pfeffer, *J. Comp. Chem.* **11**, 236 (1990).

[9] B. G. Sumpter, C. Getino, and D. W. Noid, Adv. Phys. Chem. **45**, 439-481 (1994); B. G. Sumpter and D. W. Noid, Die Makromolekulare Chemie: Theory and Simulation **3**, 363-378 (1994).

[10] R. C. Merkle, *Nanotechnology* **4**, 86 (1993).

[11] R. E. Tuzun, D. W. Noid, and B. G. Sumpter 1994, *Nanotechnology* [in press].

[12] T. W. Ebbesen, *Annu. Rev. Mater. Sci.* **24**, 235 (1994).

[13] R. E. Tuzun, D. W. Noid, and B. G. Sumpter 1994, *Nanotechnology* [in press].

[14] D. W. Noid, M. L. Koszykowski, and R. A. Marcus, *Chem. Phys. Lett.* **51**, 540 (1977); D. W. Noid, J. R. Stine, J. D. McDonald 1979, *Chem. Phys. Lett.* **65**, 153 (1977).

[15] B. G. Sumpter and D. W. Noid, *J. Chem. Phys.* **102**, 6619 (1995).

[16] R. E. Tuzun, D. W. Noid, B. G. Sumpter, and R. Merkle, 1994, *Nanotechnology* [to be submitted].

[17] R. E. Tuzun, D. W. Noid, B. G. Sumpter, and R. Merkle, 1994, *Nanotechnology* [to be submitted].

DISCLAIMER

DISCLAIMER